Limitations of high-order transformation and incident angle on simplified invisibility cloaks

Zhang, Baile; Chen, Hongsheng; Wu, Bae-Ian

2008

Zhang, B., Chen, H., & Wu, B. I. (2008). Limitations of high-order transformation and incident angle on simplified invisibility cloaks. Optics Express, 16(19), 14655-14660.

https://hdl.handle.net/10356/95035

https://doi.org/10.1364/OE.16.014655

Limitations of high-order transformation and incident angle on simplified invisibility cloaks

Baile Zhang[1*], **Hongsheng Chen**[1,2] **and Bae-Ian Wu**[1,2]

1. Research Laboratory of Electronics, Massachusetts Institute of Technology, Cambridge, MA 02139, USA.

2. The Electromagnetics Academy at Zhejiang University, Zhejiang University, Hangzhou 310058, China.

bzhang@mit.edu

Abstract: We studied the scattering from the simplified cylindrical cloaks analytically at both normal and oblique incidences. We found that these simplified cylindrical cloaks may produce a larger scattering at nonnormal incidences than that from an object without any cloak, making this object more "visible". Even at normal incidence, the high-order transformation with impedance matched at the outer boundary can produce stronger scattering than the linear simplified one without matched impedance. This is due to the inefficiency of guided waves close to the inner boundary. Therefore, a square root transformation can improve scattering by guiding waves away from the inner boundary.

OCIS codes: (230:3205) Invisibility cloaks; (290:5839) Scattering, invisibility

References and links

1. A. Alu and N. Engheta, "Achiveing transparency with plasmonic and metamaterial coatings," Phys. Rev. E **72,** 016623 (2005).
2. G. W. Milton and N. A. P. Nicorovici, "On the cloaking effects associated with anomalous localized resonance," Proc. R. Soc. London A **462,** 3027 (2006).
3. A. Sihvola, "Peculiarities in the dielectric response of negative-permittivity scatterers," Prog. Electromagn. Res. **pier-66,** 191–198 (2006).
4. N. A. P. Nicorovici, G. W. Milton, R. C. McPhedran, and L. C. Botten, "Quasistatic cloaking of two-dimensional polarizable discrete systems by anomalous resonance," Opt. Express **15,** 6314–6323 (2006).
5. A. Greenleaf, M. Lassas, and G. Uhlmann, "Anisotropic conductivities that cannot be detected by EIT," Physiol. Meas. **24,** 413–419 (2003).
6. J. B. Pendry, D. Schurig, and D. R. Smith, "Controlling Electromagnetic Fields," Science **312,** 1780–1782 (2006).
7. U. Leonhardt, "Optical Conformal Mapping," Science **312,** 1777–1780 (2006).
8. D. Schurig, J. B. Pendry, and D. R. Smith, "Calculation of material properties and ray tracing in transformation media," Opt. Express **14,** 9794–9804 (2006).
9. S. A. Cummer, Bogdan-Ioan Popa, David Schurig, D. R. Smith, and J. B. Pendry, "Full-wave simulations of electromagnetic cloaking structures," Phys. Rev. E **74,** 036621 (2006).
10. F. Zolla, S. Guenneau, A. Nicolet, and J. B. Pendry, "Electromagnetic analysis of cylindrical invisibility cloaks and the mirage effect," Opt. Lett. **32,** 1069-1071 (2007).
11. C. Blanchard, J. Porti, B. I. Wu, J. A. Morente, A. Salinas, and J. A. Kong, "Time domain simulation of electromagnetic cloaking structures with TLM method," Opt. Express **16,** 6461–6470 (2008).
12. H. Chen, B. I. Wu, B. Zhang, and J. A. Kong, "Electromagnetic Wave Interactions with a Metamaterial Cloak," Phys. Rev. Lett. **99,** 063903 (2007).
13. B. Zhang, H. Chen, B. I. Wu, Y. Luo, L. Ran, and J. A. Kong, "Response of a cylindrical invisibility cloak to electromagnetic waves," Phys. Rev. B **76,** 121101(R) (2007).

14. Z. Ruan, M. Yan, C. W. Neff, and M. Qiu, "Ideal Cylindrical Cloak: Perfect but Sensitive to Tiny Perturbations," Phys. Rev. Lett. **99,** 113903 (2007).
15. D. Schurig, J. J. Mock, B. J. Justice, S. A. Cummer, J. B. Pendry, A. F. Starr, and D. R. Smith, "Metamaterial Electromagnetic Cloak at Microwave Frequencies," Science **314,** 977–980 (2006).
16. B. Zhang, H. Chen, B. I. Wu, and J. A. Kong, "Extraordinary Surface Voltage Effect in the Invisibility Cloak with an Active Device Inside," Phys. Rev. Lett. **100,** 063904 (2008).
17. W. Cai, U. K. Chettiar, A. V. Kildishev, and V. M. Shalaev, "Optical cloaking with metamaterials," Nat. Photonics **1,** 063904 (2007).
18. W. Cai, U. K. Chettiar, A. V. Kildishev, V. M. Shalaev, and G. W. Milton, "Nonmagnetic cloak with minimized scattering," Appl. Phys. Lett. **91,** 111105 (2007).
19. Y. Huang, Y. Feng, and T. Jiang, "Electromagnetic cloaking by layered structure of homogeneous isotropic materials," Opt. Express **15,** 11133–11141 (2007).
20. H. Chen, Z. Liang, P. Yao, X. Jiang, H. Ma, and C. T. Chan, "Extending the bandwidth of electromagnetic cloaks," Phys. Rev. B **76,** 241104(R) (2007).
21. M. Yan, Z. Chao, and M. Qiu, "Cylindrical Invisibility Cloak with Simplified Material Parameters is Inherently Visible," Phys. Rev. Lett. **99,** 233901 (2007).
22. M. Yan, Z. Chao, and M. Qiu, "Scattering characteristics of simplified cylindrical invisibility cloaks," Opt. Express **15,** 17772–17782 (2007).
23. W. Cai, U. K. Chettiar, A. V. Kildishev, and V. M. Shalaev, "Designs for optical cloaking with high-order transformations," Opt. Express **16,** 5444–5452 (2008).
24. M. Farhat, S. Guenneau, A. B. Movchan, and S. Enoch, "Achieving invisibility over a finite range of frequencies," Opt. Express **16,** 5656–5661 (2008).
25. S. Xi, H. Chen, B. I. Wu, B. Zhang, J. Huangfu, D. Wang, and J. A. Kong, "Effects of different transformations on the performance of cylindrical cloaks," J. Electrom. Waves and Appl. **22,** 1489–1497 (2008).
26. A. Greenleaf, Y. Kurylev, M. Lassas, and G. Uhlmann, "Improvement of cylindrical cloaking with the SHS lining," Opt. Express **15,** 12717–12734 (2007).
27. W. C. Chew, *Waves and Fields in inhomogeneous Media,* 2nd ed, (IEEE Press, 1995).

1. Introduction

Recently there is increased interest in studying invisibility cloaks [1-26]. Methods utilizing plasmonic and negative refractive index materials were proposed to achieve invisibility by canceling the dipole moments of small objects to be concealed [1-4]. Inspired by the concept of coordinate transformation, some other methods have also been proposed [5-7]. Especially, the transformation based models proposed in Ref. [6] has been proved to be able to conceal perfectly not only passive objects [12-14], but also active sources [16] from external electromagnetic detection. In studies of the transformation based invisibility cloaks, simplified cylindrical cloaks for normally incident waves with only one polarization are often preferred in experimental demonstration [15], simulations [9, 11] and other practical designs [17-20, 23, 24]. However, the scattering evaluation at only one incident angle is not sufficient to describe the performance of such simplified cloaks. Previously, scattering results for normal incidence were obtained only semi-analytically from commercial simulation tools [21, 22]. Therefore, a fully analytic method to evaluate the performance of simplified cylindrical cloaks at both normal and oblique incidences is needed in designing invisibility cloaks.

The main reasons for scattering from a simplified cloak are the mismatches at the outer and inner boundaries. There was study on the mismatch at the outer boundary that showed that impedance matching at the outer boundary applied by a high-order quadratic transformation in Ref. [18] is able to decrease the scattering efficiently, while there is little study on the mismatch at the inner boundary.

In this paper, the field solutions of the simplified cylindrical cloaks at both normal and oblique incidences are found. The reduced scattering from these simplified cloaks can be achieved only within a limited range of incident angles. The high-order transformation with impedance matched at the outer boundary may produce stronger scattering than the simplified linear one without impedance matched at the outer boundary due to inefficiency of guided waves close to the inner boundary.

2. Scattering model and analytic algorithm

The configuration of scattering from a cylindrical cloak with outer radius R_2 and inner radius R_1 follows that in Ref. [13] where a time harmonic plane wave $\overline{E}_i = (\hat{v}_i E_{vi} + \hat{h}_i E_{hi}) e^{i\overline{k}_i \cdot \overline{r}}$ is incident with $\overline{k}_i = \hat{x}k_\rho + \hat{z}k_z$, $k_i^2 = \omega^2 \mu_0 \varepsilon_0$, $\hat{h}_i = \frac{\hat{z}\times\hat{k}_i}{|\hat{z}\times\hat{k}_i|}$ and $\hat{v}_i = \hat{h}_i \times \hat{k}_i$. In this paper we only consider incident waves with vertical polarization, i.e. $E_{hi} = 0$. Another point here is that the cloak layer between R_1 and R_2 with permittivity tensor $\overline{\overline{\varepsilon}} = \varepsilon_\rho \hat{\rho}\hat{\rho} + \varepsilon_\phi \hat{\phi}\hat{\phi} + \varepsilon_z \hat{z}\hat{z}$ and permeability tensor $\overline{\overline{\mu}} = \mu_\rho \hat{\rho}\hat{\rho} + \mu_\phi \hat{\phi}\hat{\phi} + \mu_z \hat{z}\hat{z}$ is a simplified cylindrical cloak. Without loss of generality, we assume that the concealed region of $\rho < R_1$ is a perfect electric conductor (PEC). We denote $\alpha = \pi/2 - \theta_i$ as the incident angle such that $\alpha = 0$ corresponds to the normal incidence.

In the region of $\rho > R_2$, we use scalar potentials ψ_{TM}^z and ψ_{TE}^z to describe the TE^z and TM^z harmonic cylindrical waves [13]. In the following, we will derive the state propagator matrix in the cloak shell using state-variable approach [27]. We denote $\overline{E} = \overline{E}_\rho + \overline{E}_s$ and $\overline{H} = \overline{H}_\rho + \overline{H}_s$, where $\overline{E}_\rho$ and $\overline{H}_\rho$ are components parallel to $\hat{\rho}$ while $\overline{E}_s$ and $\overline{H}_s$ are components perpendicular to $\hat{\rho}$, and $\nabla\times = \nabla_s \times + \nabla_\rho \times$, where

$$\nabla_s \times = \begin{bmatrix} 0 & \frac{-\partial}{\partial z} & \frac{\partial}{\rho\partial\phi} \\ \frac{\partial}{\partial z} & 0 & 0 \\ \frac{-\partial}{\rho\partial\phi} & 0 & 0 \end{bmatrix} \text{ and } \nabla_\rho \times = \begin{bmatrix} 0 & 0 & 0 \\ 0 & 0 & \frac{-\partial}{\partial\rho} \\ 0 & \frac{\partial}{\rho\partial\rho}\rho & 0 \end{bmatrix} \tag{1}$$

Faraday's law and Ampere's law can be written as

$$\begin{gathered} \nabla_\rho \times \overline{E}_s + \nabla_s \times \overline{E}_\rho = i\omega(\mu_\phi \hat{\phi}\hat{\phi} + \mu_z \hat{z}\hat{z}) \cdot \overline{H}_s; \\ \nabla_s \times \overline{E}_s = i\omega\mu_\rho \overline{H}_\rho; \end{gathered} \tag{2}$$

$$\begin{gathered} \nabla_\rho \times \overline{H}_s + \nabla_s \times \overline{H}_\rho = -i\omega(\varepsilon_\phi \hat{\phi}\hat{\phi} + \varepsilon_z \hat{z}\hat{z}) \cdot \overline{E}_s; \\ \nabla_s \times \overline{H}_s = -i\omega\varepsilon_\rho \overline{E}_\rho. \end{gathered} \tag{3}$$

Noting that for harmonic cylindrical waves of order n, the field has $e^{in\phi}$ and $e^{ik_z z}$ dependencies, hence the state transfer equation can be deduced after eliminating E_ρ and H_ρ in Eqs. (2) and (3) as follows:

$$\frac{\partial}{\partial\rho}\begin{bmatrix} E_z \\ E_\phi \\ H_z \\ H_\phi \end{bmatrix} = \begin{bmatrix} 0 & 0 & -\frac{ink_z}{\omega\varepsilon_\rho\rho} & -i\omega\mu_\phi + \frac{ik_z^2}{\omega\varepsilon_\rho} \\ 0 & -\frac{1}{\rho} & i\omega\mu_z - \frac{in^2}{\omega\varepsilon_\rho\rho^2} & \frac{ink_z}{\omega\varepsilon_\rho\rho} \\ \frac{ink_z}{\omega\mu_\rho\rho} & i\omega\varepsilon_\phi - \frac{ik_z^2}{\omega\mu_\rho} & 0 & 0 \\ -i\omega\varepsilon_z + \frac{in^2}{\omega\mu_\rho\rho^2} & -\frac{ink_z}{\omega\mu_\rho\rho} & 0 & -\frac{1}{\rho} \end{bmatrix} \cdot \begin{bmatrix} E_z \\ E_\phi \\ H_z \\ H_\phi \end{bmatrix}. \tag{4}$$

We let the state function be the four-dimensional vector of $\overline{V} = [E_z \; E_\phi \; H_z \; H_\phi]^T$ and denote the matrix in Eq. (4) as $\overline{\overline{T}}$. We cut the cloak shell between $\rho = R_1$ and $\rho = R_2$ into N layers, each of which has thickness of $\Delta\rho$. It follows from Eq. (4) that

$$\overline{V}(\rho_{j+1}) - \overline{V}(\rho_j) = \Delta\rho \overline{\overline{T}}(\rho_j) \cdot \overline{V}(\rho_j) \tag{5}$$

Subsequently,

$$\overline{V}(R_2) = \left[\prod_{j=1}^{N} (\overline{\overline{I}} + \Delta\rho \overline{\overline{T}}(\rho_j))\right] \cdot \overline{V}(R_1) \tag{6}$$

By choosing an sufficiently large N and matching the boundary conditions at $\rho = R_1$ and $\rho = R_2$, we are able to solve the field solution for various cylindrical cloaks with continuously varying parameters.

#97852 - $15.00 USD Received 24 Jun 2008; revised 8 Jul 2008; accepted 9 Jul 2008; published 3 Sep 2008

3. Numerical results and analysis

Now we consider different transformations from virtual space ρ' to physical space ρ as follows: linear transformation as $\rho = R_1 + (R_2 - R_1)\rho'/R_2$ [6, 9]; quadratic transformation as $\rho = [1 - R_1/R_2 + (\rho' - R_2)R_1/R_2^2]\rho' + R_1$ [18, 23]; and square root transformation as $\rho = R_1 + (R_2 - R_1)\sqrt{\rho'/R_2}$. The linear transformation allows the formation of virtual space within physical space, which is compressed linearly in the radial direction during the process. In the quadratic transformation, such compression is denser near the inner boundary. In the square root transformation, such compression is denser near the outer boundary. They can form different simplified cylindrical cloaks: (a) Linear simplified cloak [9, 15, 21] with $\varepsilon_z = \varepsilon_0[R_2/(R_2 - R_1)]^2$, $\mu_\rho = \mu_0[(\rho - R_1)/\rho]^2$ and $\mu_\phi = \mu_0$; (b) Impedance matched linear simplified cloak [22] with $\varepsilon_z = \varepsilon_0 R_2/(R_2 - R_1)$, $\mu_\rho = \mu_0 R_2/(R_2 - R_1)[(\rho - R_1)/\rho]^2$ and $\mu_\phi = \mu_0 R_2/(R_2 - R_1)$; (c) Impedance matched quadratic simplified cloak [18, 23] with $\varepsilon_z = \varepsilon_0/[2R_1\rho'/R_2^2 - 2R_1/R_2 + 1]^2$, $\mu_\rho = \mu_0(\rho'/\rho)^2[2R_1\rho'/R_2^2 - 2R_1/R_2 + 1]^2$ and $\mu_\phi = \mu_0$; and (d) Impedance matched square root simplified cloak with $\varepsilon_z = \varepsilon_0 2R_2(\rho - R_1)^2/(R_2 - R_1)^3$, $\mu_\rho = \mu_0 R_2(\rho - R_1)^2/[2(R_2 - R_1)\rho^2]$ and $\mu_\phi = \mu_0 2R_2/(R_2 - R_1)$. Note that (a) and (b) are both from linear transformation and (b), (c) and (d) have matched impedance at the outer boundary [18, 22, 23].

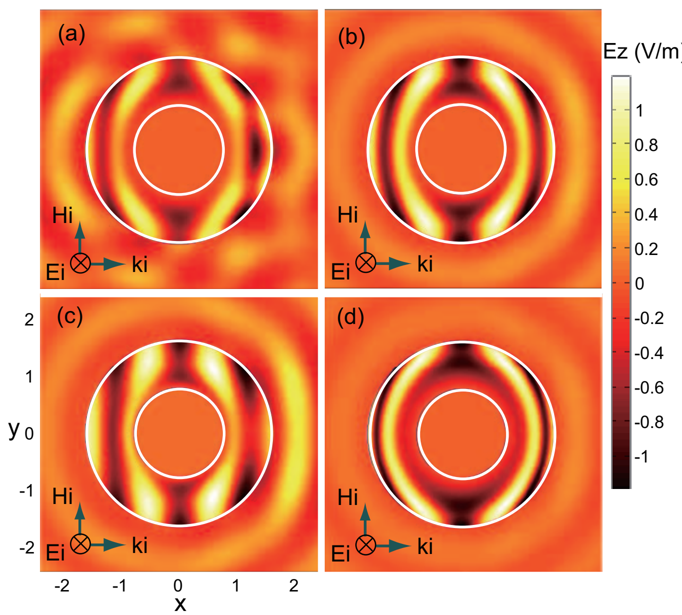

Fig. 1. (Color online) Electric field distribution of different simplified cylindrical cloaks illuminated by a vertically polarized and normally incident plane wave. Only scattered field is plotted outside of the cloak. $R_2 = 1.5\lambda_0 = 2.08R_1$. (a) Linear simplified cloak; (b) Impedance matched linear simplified cloak; (c) Impedance matched quadratic simplified cloak; (d) Impedance matched square root simplified cloak. From (a) to (d), the normalized RCS is 0.299, 0.125, 0.360 and 0.034, respectively.

Figure 1 shows the electric field distribution in *xy* plane of different simplified cylindrical cloaks illuminated by a normally incident plane wave with vertical polarization. In region $\rho > R_2$, only the scattered field is plotted. In Fig. 1(a), the linear simplified cloak has some intrinsic scattering [21], especially in the backward direction due to the impedance mismatch. From Fig. 1(a) to Fig. 1(b), the field pattern inside the cloak shell (the bending effect of waves) does

#97852 - $15.00 USD Received 24 Jun 2008; revised 8 Jul 2008; accepted 9 Jul 2008; published 3 Sep 2008

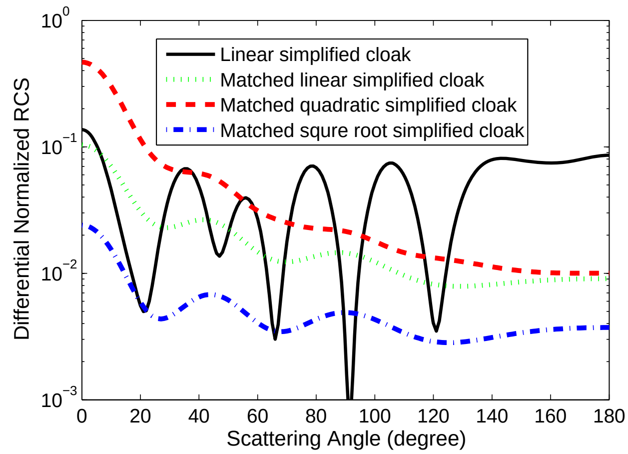

Fig. 2. (Color online) Comparison of the far-field differential normalized RCS of different simplified cylindrical cloaks illuminated by a vertically polarized and normally incident plane wave. $R_2 = 1.5\lambda_0 = 2.08R_1$.

not change much, since these cases are both from linear transformation. However, the scattered field (normalized radar cross section (RCS) Q_{scat} [13]) is reduced significantly because the impedance at the outer boundary has been matched. The ring-like scattered field pattern is mainly from the zeroth order scattering [21], which is impossible to be completely eliminated by simplified cloaks due to the lack of surface magnetic current in this case [13, 26]. When the waves reach the inner boundary, instead of inducing magnetic current along $\hat{\phi}$ direction in the case of ideal cylindrical cloak [13, 26], they induce electric current along $\hat{z}$ direction on the surface of PEC core which reradiates and contributes to scattering. From Fig. 1(b) to Fig. 1(c), the impedance at the outer boundary stays matched, but the quadratic transformation in Fig. 1(c) forces most waves to be bent close to the inner boundary. Thus, more energy of the incident waves is blocked by the PEC core in Fig. 1(c) than in Fig. 1(b), forming a shadow behind the cloak characterized by a strong forward scattering as shown in Fig. 1(c). It is worth noting that the normalized RCS in Fig. 1(c) is even larger than that in Fig. 1(a). This result does not contradict with that in Ref. [18], since in the case studied in Ref. [18], the surface electric current on the PEC core happens to be helpful for complete cloaking [13, 26]. In Fig. 1(d), the square root transformation forces most waves to be bent away from the inner boundary and thus produces a very small RCS. Figure 2 shows the far-field differential normalized RCS [13] of cases (a) to (d) in Fig. 1. It can be seen that all the simplified cloaks having matched impedance at the outer boundary are able to suppress the backward scattering efficiently. But the impedance matched quadratic simplified cloak has so large forward scattering which leads to an even larger total RCS, while the impedance matched square root simplified cloak is able to suppress both backward and forward scattering, which therefore results in the smallest total RCS.

We can further calculate the scattering at nonnormal incidences. For each simplified cloak, since only ε_z, μ_ρ and μ_ϕ are specified, we require that $\mu_z/\mu_0 = \varepsilon_z/\varepsilon_0$, $\varepsilon_\rho/\varepsilon_0 = \mu_\rho/\mu_0$ and $\varepsilon_\phi/\varepsilon_0 = \mu_\phi/\mu_0$. As shown in Fig. 3, the reduced RCS can only be achieved within a limited range of incident angles, beyond which the scattering is even larger than a bare PEC without any cloak. This result is reasonable since the simplified cloaks are all designed for only normal incidence while the scattering performance at other incident angles has not been considered. Therefore it can be expected that as the incident angle increases, the scattering will increase. But

#97852 - $15.00 USD Received 24 Jun 2008; revised 8 Jul 2008; accepted 9 Jul 2008; published 3 Sep 2008

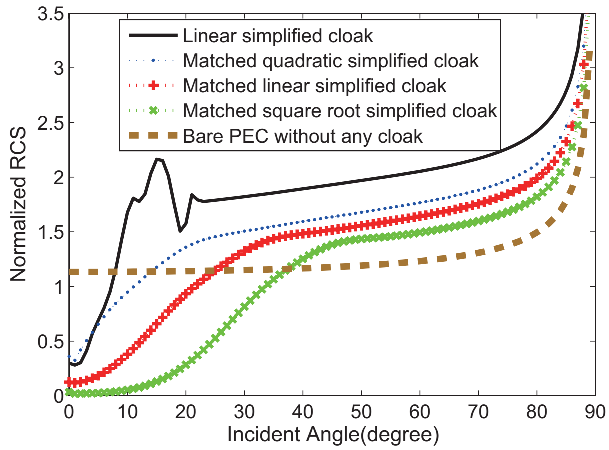

Fig. 3. (Color online) Dependance of normalized RCS (normalized to $2R_2$) on incident angles for different simplified cloaks. $R_2 = 1.5\lambda_0 = 2.08R_1$.

an important question is what is the critical incident angle beyond which a simplified invisibility cloak no longer makes an object "invisible" but makes it even more "visible". Obviously, this critical incident angle is of great importance in practical applications of simplified invisibility cloaks.

4. Conclusion

In summary, we calculated the scattering from the simplified cylindrical cloaks at both normal and oblique incidences. We found that simplified cylindrical cloaks may produce a larger scattering at nonnormal incidences than that from an object without any cloak. The impedance matched high-order transformation forces waves to be bent close to the inner boundary and thus may produce stronger scattering than the simplified linear one without impedance matched at the outer boundary.

Acknowledgments

This work is sponsored by ONR under Contract N00014-01-1-0713, the Department of the Air Force under Air Force Contract F19628-00-C-0002, and the Chinese NSF under Grant No. 60531020.

#97852 - $15.00 USD Received 24 Jun 2008; revised 8 Jul 2008; accepted 9 Jul 2008; published 3 Sep 2008